Title

Mechanism-based corrector combination restores ΔF508-CFTR folding and function

Journal

Nature Chemical Biology, 9(7)

ISSN

1552-4450

Authors

Okiyoneda, Tsukasa
Veit, Guido
Dekkers, Johanna F
et al.

Publication Date

2013-07-01

DOI

10.1038/nchembio.1253

Peer reviewed

Published in final edited form as:
Nat Chem Biol. 2013 July ; 9(7): . doi:10.1038/nchembio.1253.

Mechanism-based corrector combination restores ΔF508-CFTR folding and function

Tsukasa Okiyoneda[1,11], **Guido Veit**[1], **Johanna F. Dekkers**[2,3,4], **Miklos Bagdany**[1], **Naoto Soya**[1], **Haijin Xu**[1], **Ariel Roldan**[1], **Alan S. Verkman**[5], **Mark Kurth**[6], **Agnes Simon**[7], **Tamas Hegedus**[8], **Jeffrey M. Beekman**[2,3,4], and **Gergely L. Lukacs**[1,9,10]

[1]Department of Physiology, McGill University, Montréal, Quebec H3G 1Y6, Canada [2]Department of Pediatric Pulmonology, University Medical Centre, Utrecht, The Netherlands [3]Department of Immunology, University Medical Centre, Utrecht, The Netherlands [4]Centre for Molecular and Cellular Intervention, University Medical Centre, Utrecht, The Netherlands [5]Departments of Medicine and Physiology, University of California San Francisco, San Francisco [6]Department of Chemistry, University of California Davis, Davis, California [7]Department of Molecular Pharmacology, Research Center for Natural Sciences, Hungarian Academy of Sciences, Budapest, Hungary [8]MTA-SE Molecular Biophysics Research Group and Department of Biophysics and Radiation Biology, Semmelweis University, Budapest, Hungary [9]Department of Biochemistry, McGill University, Montréal, Quebec H3G 1Y6, Canada [10]GRASP, McGill University, Montréal, Quebec H3G 1Y6, Canada

Abstract

The most common cystic fibrosis (CF) mutation, ΔF508 in the nucleotide binding domain-1 (NBD1), impairs CFTR coupled-domain folding, plasma membrane (PM) expression, function and stability. VX-809, a promising investigational corrector of ΔF508-CFTR misprocessing, has limited clinical benefit and incompletely understood mechanism, hampering drug development. Based on the effect of second site suppressor mutations, robust ΔF508-CFTR correction likely requires stabilization of NBD1 and the membrane spanning domains (MSDs)-NBD1 interface, both established primary conformational defects. Here, we elucidated the molecular targets of available correctors; class-I stabilizes the NBD1-MSD1/2 interface, class-II targets NBD2, and only chemical chaperones, surrogates of class-III correctors, stabilize the human ΔF508-NBD1. While VX-809 can correct missense mutations primarily destabilizing the NBD1-MSD1/2 interface, functional PM expression of ΔF508-CFTR also requires compounds that counteract the

Correspondence should be addressed to: G. L. Lukacs, Department of Physiology, McGill University, 3655 Promenade Sir-William-Osler, Montreal, Quebec H3G 1Y6, Canada, gergely.lukacs@mcgill.ca, Ph: 514-398-5582.
[11]Current address: Department of Bioscience, School of Science and Technology, KwanseiGakuin University, Sanda, Hyogo 669-1337, Japan

Author Contributions

T.O. designed and carried out the biochemical studies, including the cell surface ELISA, pulse-chase and immunoblotting assays and analysed the data. G.V. generated the inducible epithelial cell lines and carried out the apical chloride current measurements, J.F.D. performed the intestinal organoid transport assay under the direction of J.M.B., M.B. carried out the bilayer measurements, N.S. measured the HDX of NBDs, H.X. engineered the CFTR mutants and generated the BHK cell lines, A.R. purified the NBDs and characterized their thermal stability, A.S.V. and M.K. provided reagents, A.S. and T.H. performed the in silico docking, G.L.L. conceived and directed the study, and wrote the manuscript with T.O.

Competing financial interests

The authors declare no competing financial interests.

Supplementary information is available in the online version of the paper.

NBD1 and NBD2 stability defects in CF bronchial epithelial cells and intestinal organoids. Thus, structure-guided corrector combination represents an effective approach for CF therapy.

Cystic fibrosis transmembrane conductance regulator (CFTR) is an ATP-binding cassette transporter and functions as a cAMP-dependent Cl^- channel at the apical plasma membrane (PM) of epithelial cells[1]. CFTR comprises two membrane spanning domains (MSD1, MSD2) with four cytosolic loops (CL1-4), and three cytosolic domains: a regulatory (R) and two nucleotide-binding domains (NBD1, NBD2). CFTR domain swapped architecture forms multiple domain-domain interfaces that appear to be critical in the channel structural and functional integrity[2–4] (Fig. 1a). Newly synthesized CFTR is N-glycosylated and undergoes co-translational domain folding and post-translational, coupled-domain assembly in the ER[2,5–9], aided by a network of molecular chaperones[10,11] (Supplementary Fig. 1a). Upon bypassing the ER quality control checkpoints and traversing the Golgi complex, the native CFTR undergoes complex-glycosylation[1,11].

CF, one of the most common inherited disease in the Caucasian population, is caused by loss-of-function mutations of CFTR that lead to the imbalance of airway surface fluid homeostasis, mucus dehydration, hyperinflammation, bacterial colonization, and consequently recurrent lung infection, the primary cause of morbidity and mortality in CF[1,12,13]. Deletion of F508 (ΔF508) in the NBD1, the most prevalent CFTR mutation present in ~90% of CF patients, causes global misfolding and ER associated degradation (ERAD) via the ubiquitin proteasome system, resulting in marginal PM expression of the partially functional ΔF508-CFTR[1,6,11,14]. The residual PM channel activity could be enhanced by modulating the ΔF508-CFTR biosynthetic processing, peripheral stability, and channel gating by low temperature, chemical chaperones or small molecules[14–19].

While symptomatic therapies have increased the life expectancy of CF patients, considerable efforts have been devoted to identify compounds that can increase either the mutant biosynthetic processing efficiency and cell surface density (“correctors”) or the activity of PM resident mutant CFTR (“potentiators”)[19]. VX-770 (Ivacaftor), the only approved potentiator drug, substantially enhances the channel function of several mutants[20], as opposed to available “correctors” that are modestly effective with incompletely understood mechanism[14,17,21]. In principle, correctors may facilitate ΔF508-CFTR folding via direct binding as pharmacological chaperones (PC)[22], or indirectly, as chemical chaperones (CC, e.g. glycerol, TMAO and myo-inositol)[16,23]. Correctors may also enhance the mutant functional expression as proteostasis regulators (PR)[11] by modulating the cellular machineries responsible for folding, degradation, and vesicular trafficking of ΔF508-CFTR (e.g. 4-phenylbutyrate, HDAC inhibitor, HSF1-inducers and kinase inhibitors, see for review[11,19]). VX-809, the most promising investigational corrector, restores the mutant PM expression and function to <15% of WT-CFTR in immortalized and primary human bronchial epithelia[14]. Although circumstantial evidence suggests that VX-809, similarly to some of the previously identified correctors (e.g. C3 [VRT-325] and C4 [corr-4a]) and potentiators (e.g. P1 [VRT-532] and VX-770), directly targets ΔF508-CFTR during ER biogenesis, the molecular basis of correction remains elusive[14,24]. While the VX-809-induced ΔF508-CFTR activity is potentiated by two fold with VX-770 at the PM in preclinical settings[14], additional improvement seems to be required in corrector efficacy to achieve substantial clinical benefit in CF[21].

Recent studies revealed that the ΔF508-NBD1 is thermodynamically and kinetically destabilized at physiological temperature and suggested that NBD1 stabilization would effectively counteract ΔF508-CFTR misprocessing[25,26]. Substantial stabilization of the ΔF508-NBD1 by suppressor mutations, however, resulted in a limited increase in folding and PM expression of the ΔF508-CFTR[27,28]. Remarkably, robust rescue (65–80%) of

ΔF508-CFTR folding could be achieved by suppressor mutations that simultaneously stabilized the ΔF508-NBD1, as well as the NBD1 interface with the CL4 coupling helix in the MSD2[27,28]. These observations suggest that efficient correction of both primary structural defects is necessary and sufficient to restore ΔF508-CFTR function close to WT level in most CF patients. As a corollary, it is conceivably that correction of one of the primary (NBD1 or the NBD1-MSD2 interface) or a secondary structural defect (e.g. NBD2 misfolding[5]) accounts for the ΔF508-CFTR limited rescue efficiency by correctors identified to date[11,14,17,19,21,22,29]. Furthermore, combinations of correctors that counteract distinct conformational defects may potentiate each other effect on ΔF508-CFTR folding and function in analogy to suppressor mutations of the primary folding defects[27,28] (Supplementary Fig. 1b).

Based on *in vitro* studies of isolated ΔF508-NBD1 in combination with *in vivo* CFTR processing, functional assays, and *in silico* docking analysis, as well as published data[22], here we propose that correctors can be mechanistically classified into three groups. We also show that the efficacy of VX-809, targeting the NBD1-MSD1/2 interface, can be significantly potentiated with two other classes of chemicals, as determined by ΔF508-CFTR folding, PM expression, stability, and function in cell culture models and intestinal organoids from CF patients. Thus, targeting multiple conformational defects enables us to counteract ΔF508-CFTR misfolding, demonstrating that structure-guided corrector combination may provide an effective therapeutic strategy in CF.

Result

Class-I corrector plus NBD1 stabilization restore folding

We postulated that small molecule combinations targeting both primary folding defects would achieve WT-like folding of ΔF508-CFTR as documented in case of second site suppressor mutations[27,28]. To categorize the available corrector molecules (Supplementary Results, Supplementary Table 1) according to their preferential targets, we determined the rescue efficiency of ΔF508-CFTR containing either the genetically stabilized NBD1 (by R1S mutation: G550E, R553Q, R555K and F494N; second site mutations are defined in Supplementary Table 2) or the stabilized NBD1-MSD2 interface (by the R1070W mutation in the CL4) (Fig. 1a). We confirmed that the R1070W or R1S suppressor mutation modestly increased the ΔF508-CFTR PM density from <2 % to 7 or 16% of the WT level, respectively, determined by cell surface ELISA in BHK cells[27] (Supplementary Fig. 2a). VX-809, C18 (a VX-809 analogue) or C3, the most effective correctors in our screen, increased the PM density of ΔF508-CFTR-R1S and ΔF508-CFTR-R1070W to 93–100% and 30–34% of the WT, respectively (Fig. 1b). This suggests that VX-809, C18 and C3 preferentially target the NBD1/MSD2 interface over the NBD1 energetic defect and they were designated as class-I correctors (Fig. 1b and Supplementary Fig. 2a). The preferential rescue of the NBD1-MSD2 interface and NBD1 stability defects was estimated by the augmented PM density of ΔF508-CFTR-R1S (Res_{R1S}) and ΔF508-CFTR-R1070W (Res_{R1070W}), respectively, a measure that indicates the capacity of correctors to synergize with the respective suppressor mutation (Supplementary Fig. 2a). The ratio of Res_{R1S} over Res_{R1070W} suggested that VX-809, C18 or C3 has ~3.5 fold more stronger stabilizing effect on the NBD1-MSD2 interface than on the NBD1 (Fig. 1c). This inference was confirmed by using ΔF508-CFTR variants, containing functionally analogous 3S (F494N, Q637R, and F429S) and R (G550E, R553Q, R555K) or V510D suppressor mutations that stabilize the NBD1 or the NBD1-MSD2 interface, respectively[7,27,30,31]. VX-809, C18 or C3 increased PM density of ΔF508-CFTR-3S and ΔF508-CFTR-R from 7–25% to 60–120% of WT and their complex-glycosylation, but was less effective in case of ΔF508-CFTR-V510D similar to ΔF508-CFTR-R1070W (Supplementary Fig. 2b–c). A similar difference was obtained by analyzing the magnitude of fold-correction relative to that induced by the respective second-

site mutation(s) alone. The reduced rescue efficiency of the ΔF508-CFTR-3S relative to ΔF508-CFTR-R1S by class-I correctors may be attributed to the more efficient stabilization of the NBD1-NBD2 interface with R1S suppressor mutation.

Metabolic pulse-chase experiments confirmed that only combination of VX-809, C18 or C3 with NBD1 (R1S) but not with interface stabilization (R1070W or V510D) enhanced ΔF508-CFTR folding efficiency near to the WT level (22–32%), indicating a 4–8-fold potentiation between class-I correctors and R1S mutation effect (Fig. 1d and Supplementary Fig. 2d). Dual acting compounds such as C15 (corr-2b[32]) and CoPo-22 (CoPo[33]) combining corrector and potentiator effect only slightly enhanced the PM density of ΔF508-CFTR variants (Supplementary Fig. 2a).

The WT-like ΔF508-CFTR complex-glycosylation, function and PM density was reproduced by genetic stabilization of NBD1 and NBD1-MSD2 interface, as well as by the combination of class-I corrector and NBD1 suppressor mutations in polarized human immortalized CF bronchial respiratory epithelial (CFBE41o-) cells (Supplementary Fig. 3). Class-I correctors increased the PM density, complex-glycosylation and apical Cl^- current (ICl(apical)) of ΔF508-CFTR to ~100–130 % and ~30 % of the WT level in the presence of R1S and R1070W, respectively, in CFBE41o- cells expressing the mutant channel under the control of tetracycline responsive promoter (Fig. 1e–f and Supplementary Fig. 3e–g), consistent with preferential stabilization of the NBD1-MSD2 interface by class-I correctors in CFBE41o- cells.

To evaluate the efficiency of class-I corrector as a function of the ΔF508-NBD1 conformational stability, the relationship between NBD1 stability (reflected by the T_m values of 0S, 1S [F494N], 3S or R4S suppressor mutant of ΔF508-NBD1 or WT-NBD1, listed in Supplementary Table 2) and PM density of the respective CFTR variants was established. The WT-CFTR PM expression was dependent on the NBD1 stability at an 8-fold steeper slope (12.9 ± 3.1 %/°C), as compared to that of ΔF508-CFTR (1.7 ± 0.2 %/°C), confirming the critical role of the F508 side chain in CFTR coupled domain folding[1,6] (Fig. 1g). Similar to the R1070W mutation[27] (9.2 ± 2.3 %/°C), VX-809 (9.8 ± 0.7 %/°C), C18 (9.6 ± 1.3 %/°C) or C3 (10.8±2.1 %/°C) restored WT-like coupling between NBD1 stability (T_m) and ΔF508-CFTR PM expression, supporting the possibility that class-I correctors stabilize the NBD1-MSD2 interface (Fig. 1g). Interestingly, the improvement of WT-CFTR PM expression by NBD1 stabilization reinforces the notion that the inherent conformational fluctuation of the NBD1 partly accounts for limited processing efficiency of the WT channel[27] (Fig. 1g).

Mechanisms of action of CFTR correction

To assess whether VX-809 or C18 can directly bind to ΔF508-CFTR as a PC, the functional stability of the temperature-rescued mutant channel was determined in artificial planar phospholipid bilayer[27,34]. These experiments used the ΔF508-CFTR-2RK, incorporating R29K and R555K mutations to improve the channel reconstitution success by modestly enhancing the PM expression after the 26°C rescue while preserving the ΔF508-CFTR channel gating and functional stability defects as reported before[34] (Supplementary Fig. 4a–c). The open probability (P_o) of the phosphorylated ΔF508-CFTR-2RK channel was progressively decreased from 0.21 to 0.09 upon raising the temperature from 24°C to 36°C[34,35] (Fig. 2a–b). In contrast, the P_o of the WT was increased from 0.35 to 0.47 (Fig. 2a–b). VX-809 and C18 prevented the mutant thermal inactivation and maintained the P_o = 0.21 and 0.26, respectively, at 36°C during the course of the measurement (Fig. 2a–b and Supplementary Fig. 4d), providing evidence that these compounds can directly interact with the channel.

To delineate potential VX-809 target sites, *in silico* docking was performed on the NBD1 crystal structure (PDB:2BBT) and two CFTR homology models[3,36] following the deletion of the F508 using AutoDock. VX-809 was docked to NBD1-CL1(MSD1), NBD1-CL4(MSD2), and NBD1-NBD2 interfaces (Fig. 2c, Supplementary Fig. 5 and Table 3). Some of these sites have been reported as putative corrector binding sites[37,38]. To test the *in silico* predictions, the NBD1-CL4 and NBD1-CL1 interfaces were disrupted by R1070W or F508G[5,6,27,39] and the CF-causing R170G mutation (http://www.genet.sickkids.on.ca/app), respectively, in WT CFTR. The R170G substitution probably disrupts the electrostatic interaction between R170 (CL1) and E402, E403 and/or E476 (NBD1) (Fig. 1a). The F508G interferes with the hydrophobic patch formation at the NBD1-CL4 interface while only marginally compromises the NBD1 energetics[3,27]. These events lead to the destabilization of the joint CL1/CL4 interface with NBD1 and subsequent misfolding of multiple CFTR domains[6]. Remarkably, the severe processing and PM expression defects of both CL1 and CL4 interface mutants were largely corrected by VX-809, C18 or C3 (Fig. 3a–c). Conversely, stabilizing the NBD1-CL4 interface by V510D or R1070W mutation in the absence of F508 attenuated the relative efficiency of class-I correctors but not of C4 on ΔF508-3S-CFTR (Fig. 3d and Supplementary Fig. 6a). Moreover, V510D mutation which improves the WT expression conceivably by stabilizing the NBD1-CL4/CL1 interface and marginally the NBD1 itself[27], also attenuated the effect of class-I correctors on WT CFTR (Supplementary Fig. 6b). Surprisingly, V510D but not the R1S mutation, substantially corrected the R170G defect (Supplementary Fig. 6c), suggesting that the NBD1-CL1 interface defect is coupled to that of the NBD1-CL4. The rescue of R170G-CFTR expression by class-I correctors, however, was partially diminished by the V510D mutation (Supplementary Fig. 6d). In addition to *in silico* docking prediction (Supplementary Fig. 5a, c and e), the stronger effect of VX-809 on the CL1 mutants compared to transmembrane (TM) helix 1 mutants, such as G85E and G91R (Supplementary Fig. 7a), also consistent with the model that VX-809 targets the interdomain interface composed of NBD1 and the CL1/CL4, containing the respective coupling helices[1].

To further dissect the VX-809 target, we assessed its effect on the steady-state expression of WT CFTR domain combinations, representing stalled biosynthetic folding intermediates[6,40]. This approach is favored by the observation that the conformation of early folding intermediates is similar between WT and ΔF508-CFTR[41]. VX-809 increased the level of WT and ΔF508 MSD1-NBD1 (M1N1) equally, as well as the WT MSD1 and MSD1-NBD1-R, but not the domain combinations that lacked MSD1 (Supplementary Fig. 7a–e), suggesting that VX-809 may target MSD1 and stabilize the domain interface composed of CL1/CL4.

To determine the possible role of VX-809 at the NBD1-NBD2 interface, NBD2 deletion mutants (CFTR-ΔNBD2) were used considering the similar folding characteristics of WT and CFTR-ΔNBD2[6–8]. Class-I correctors and the R1S mutation rescued the ΔF508-CFTR-ΔNBD2 PM expression to 50–75 % of its WT counterpart as in the case of the full-length molecule (Fig. 3e–f), ruling out a significant role of NBD1-NBD2 or NBD2-MSDs interfaces in the CFTR correction (Supplementary Fig. 5c–f). This result was in agreement with the prediction of preserved VX-809 binding sites on the CFTR-ΔNBD2 model (Fig. 2c). In contrast, NBD2 deletion virtually eliminated the ΔF508-CFTR-R1S correction by C4 (a C13 analogue)[17] or core-corr-II[42] (Fig. 3e–f). Therefore, we designated C4 and core-corr-II as members of class-II correctors (Fig. 1b–c and Supplementary Fig. 2a). Preventing class-II corrector effect by the NBD2 deletion is consistent with *in silico* docking predictions, supporting that the putative target of C4 and core-corr-II is the NBD1-NBD2 and/or NBD2-MSD1/2 interface (Supplementary Fig. 8–9), and with the weaker rescue efficiency of class-II correctors on the NBD1-MSD1/2 interface mutants (R1070W, F508G or R170G) compared to that of class-I correctors (Fig. 3a–c). These results are also in line

with the observation that the C4 rescue effect is exerted only after the completion of MSD2 translation[40]. Although *in silico* docking predicted the regulatory insertion (RI)[43] as a possible binding site of class-II correctors in NBD1 (Supplementary Fig. 8–9), this scenario was ruled out because C4 remained effective for the ΔF508-CFTR-ΔRI containing energetically stabilized NBD1[25,26] (Supplementary Fig. 9f).

Chemical chaperones stabilize the human ΔF508-NBD1

Although none of the correctors tested appears to preferentially stabilize the NBD1 according to the structural complementation analysis (Fig. 1b–c), it remains possible that correctors can exert limited conformational stabilization effect on the human ΔF508-NBD1 similar to that of RDR1 on the mouse ΔF508-NBD1[22]. To assess this possibility, first the thermal unfolding propensity of the domain was monitored by differential scanning fluorimetry (DSF)[27]. Initial studies were carried out on the human ΔF508-NBD1 containing a single solubilizing mutation F494N (ΔF508-NBD1-1S), followed by validation on the native ΔF508-NBD1 with significantly reduced protein yield and increased thermal sensitivity. Most of the available correctors including RDR1[22], failed to counteract the conformational instability of the human ΔF508-NBD1-1S and ΔF508-NBD1, reflected by their <8~9°C lower melting temperature (T_m) relative to their WT counterparts (Fig. 4a–c and Supplementary Fig. 10a). C6, C11 (dynasore) or C12 weakly increased the T_m of ΔF508-NBD1-1S but this effect was minimal on the ΔF508-NBD1 (Fig. 4b–c and Supplementary Fig. 10a). Accordingly, C11 neither attenuated the *in vitro* ubiquitination of the unfolded NBD1 by the chaperone-dependent E3 ubiquitin ligase CHIP[27] (Supplementary Fig. 10b) nor enhanced the PM expression of the CD4T-ΔF508-NBD1-1S chimera (see below). In contrast, ATP and chemical chaperones (CCs; glycerol, TMAO, myo-inositol and D-sorbitol) substantially enhanced the T_m of ΔF508-NBD1-1S and ΔF508-NBD1 (Fig. 4a–c and Supplementary Fig. 10a). The DSF results were substantiated by monitoring the NBD1 *in vivo* folding in the context of the CD4T-ΔF508-NBD1-1S chimera. PM density measurement of the chimeras, as a validated surrogate readout of the biosynthetic processing efficiency[6,27], showed that only CCs (e.g. glycerol and myo-inositol) and solubilizing mutations (R4S) but none of the correctors stabilized the cytosolic ΔF508-NBD1-1S anchored to the truncated CD4 reporter molecule (Fig. 4d).

Considering the enhanced conformational dynamics of amino acid residues 507-511 in the isolated ΔF508-NBD1-3S shown by hydrogen deuterium exchange and mass spectrometry (HDX-MS)[44], we tested whether VX-809 can limit the conformational dynamics of this region. We confirmed the accelerated deuteration of the 505-509 amino acid peptide in ΔF508-NBD1-1S relative to its WT counterpart[44], but not of the remaining >60 peptides, representing 98% sequence coverage of NBD1-1S (Fig. 4e–h and Supplementary Fig. 10c). VX-809, however, was unable to suppress the HDX kinetics of the 505-509 segment, as well as the other peptides, suggesting that VX-809 is unable to elicit localized conformational stabilization on the ΔF508-NBD1-1S (Fig. 4e–h).

Corrector combinations robustly rescue ΔF508 in BHK cell

Based on this study and other published data[22,38,40], we propose the categorization of the ΔF508 correctors into three classes (Fig. 5a). Class-I (C3, C18 and VX-809) primarily stabilizes the NBD1-CL1/4 interface, class-II (core-corr-II and corr-4 analogues [C4, C13]) targets NBD2 and/or its interface, and class-III stabilizes the ΔF508-NBD1. Since RDR1 stabilize the mouse, but not the human NBD1[22] (Fig. 4), we used CCs, such as glycerol as surrogate class-III correctors in our proof-of-principle studies.

Combination of chemicals with complementary structural targets is predicted to potentiate the individual correctors via ΔF508-CFTR coupled domain-folding and phenocopy the

combination of suppressor mutations[27,28] (Supplementary Fig. 1b). While class-I corrector (VX-809, C18 or C3) with class-II corrector (C4 or core-corr-II) only modestly rescued ΔF508-CFTR PM level (<10% of WT CFTR), combination of class-I corrector and glycerol enhanced the ΔF508-CFTR PM expression to 30–50% of the WT, supporting that correction of both primary defects is required for the robust ΔF508-CFTR rescue (Fig. 5b). The class-I corrector or glycerol effect that individually achieved <8% rescue was further improved by class-II correctors and enhanced the ΔF508-CFTR PM expression to ~60–110% of WT (Fig. 5b). Similar phenotypes were confirmed by monitoring the accumulation of complex-glycosylated ΔF508-CFTR with immunoblotting (Fig. 5c). Metabolic pulse-chase experiments (Fig. 5d–e) and ELISA (Fig. 5f) revealed that the combined treatment increased the ΔF508-CFTR folding efficiency to ~70% of the WT and largely rescued the mutant PM stability defect. Thus, both enhanced ER folding efficiency and PM stability of ΔF508-CFTR in the presence of two classes of correctors with glycerol account for the WT-like PM expression.

ΔF508-CFTR rescue in bronchial epithelia

The rationally selected chemical combination also significantly potentiated the VX-809 rescue of the ΔF508-CFTR in polarized respiratory epithelial cells. The ΔF508-CFTR PM density in CFBE41o- cells treated with a class-I corrector was enhanced by ~3-fold in the presence of 5% glycerol that was further augmented by class-II corrector (C4 or core-corr-II), representing ~5 fold increase of the VX-809 effect (Fig. 6a). Combined treatment of two classes of correctors with glycerol enhanced the PM density of ΔF508-CFTR to ~10% of the WT CFTR level, a comparable efficacy to that achieved by low temperature (Fig. 6a). The VX-809 effect was further potentiated by combination with C4, and glycerol and partially restored the ΔF508-CFTR complex-glycosylation (Fig. 6b), PM stability (Fig. 6c), and function at the apical PM in CFBE41o- epithelia (Fig. 6d–e). Similar enhancement was observed in other polarized epithelial cell models. The combined treatment enhanced the PM density of ΔF508-CFTR to ~40% and ~15% of the WT level in Madin-Darby Canine Kidney (MDCKII) and human lung papillary adenocarcinoma epithelial cells (NCI-H441), respectively (Supplementary Fig. 11).

Functional correction of ΔF508-CFTR in CF rectal organoid

Finally, the efficacy of the mechanism-based corrector combination was evaluated in human rectal organoids derived from CF patients homozygous for the ΔF508 mutation[45]. CFTR channel activity was measured by monitoring the forskolin-induced swelling (FIS) of organoids, since the cross-sectional area of organoids was proportional with CFTR-mediated chloride and coupled water transport[45]. While class-I corrector (C18 or VX-809) modestly improved the FIS of $CFTR^{\Delta F508/\Delta F508}$ organoids, combining it with myo-inositol[46], a CC selected based on its minimal toxicity, enhanced the ΔF508-CFTR-dependent FIS to 30–60% of that observed in organoids from healthy individuals (WT) (Fig. 6f–h). The rescued ΔF508-CFTR mediated FIS was completely prevented with CFTR blockers (Inh_{172} and GlyH101) (Fig. 6f–h). Likewise, organoids expressing nonfunctional, truncated CFTR variants (E60X/4015ATTdel) also failed to display any FIS (Fig. 6h). Remarkably, VX-809, C4 and myo-inositol jointly restored the ΔF508-CFTR-dependent FIS by >80% of the WT. Comparison of individual and dual and triple combination effect of correctors on FIS of $CFTR^{\Delta F508/\Delta F508}$ organoids indicates a 2–2.5-fold potentiation (Fig. 6h). Together, these results demonstrate that mechanism-based corrector combinations are capable to robustly rescue ΔF508-CFTR folding and function in cell culture models and primary human CF organoids.

Interestingly, class-I, class-II corrector or glycerol also augmented the PM expression of WT CFTR that has an intrinsic low folding efficiency (~30%)[1] (Supplementary Fig. 12a). The

WT CFTR rescue efficiency by VX-809 or C18 but not C4 was suppressed in the presence of V510D mutation and, to a lesser extent by 3S or R4S mutation (Supplementary Fig. 12b), consistent with the limited conformational instability of the NBD1-MSDs interface and NBD1 in WT CFTR[27]. These observations with the overlapping VX-809 *in silico* docking data on ΔF508 and WT CFTR (Supplementary Fig. 12c), as well as MSD1 stabilization are consistent with the possibility that VX-809, similarly to the V510D mutation, targets the conformationally unstable WT NBD1-MSD1/2 interface.

Discussion

Here we show that combination of correctors targeting complementary conformational defects can overcome their individually modest impact and synergistically restore the ΔF508-CFTR processing and PM channel function. Using *in vivo*, *in vitro,* and *in silico* analyses, we identified subsets of correctors that preferentially target the primary conformational defect at the NBD1-MSD1(CL1)/MSD2(CL4) interface (class-I) or the consequential NBD2 misassembly (class-II). None of the tested correctors belong to class-III that targets the human ΔF508-NBD1 energetic defect. Only CCs, such as glycerol and myo-inositol, can substitute for a class-III corrector by stabilizing the human ΔF508-NBD1 both *in vitro* and *in vivo*. While we cannot rule out that glycerol has multiple targets in ΔF508-CFTR, NBD2 deletion diminished the glycerol effect on PM expression and complex-glycosylation of ΔF508-R1S-CFTR, but left the ΔF508-CFTR-R1070W expression largely unaffected (Fig. 3e–f and Supplementary Fig. 7f–g). In addition, glycerol rescued the PM level of ΔF508-CFTR-R1070W similar to that of the NBD1 stabilizing mutations[24] (Supplementary Fig. 7f–g). These observations suggest that glycerol may primarily stabilize the NBD1. The proposed corrector classification also provides a plausible explanation for the additive effect of C3 (class-I) and C4 (class-II)[47,48] or VX-809 (class-I) and C4 (class-II), the attenuated efficiency of C3 and VX-809[14] and the potentiation of class-I by CCs (as surrogate of class-III) (Fig. 5–6). The limited synergy between class-I and class-II correctors in the absence of CC may imply that suppression of ΔF508-CFTR primary defects is a prerequisite for correction of the secondary NBD2 defect.

By selectively increasing the ER folding efficiency and the PM stability in multiple cellular models, VX-809 was predicted to overcome a kinetic folding trap and/or stabilize the native-like conformer by direct interaction with ΔF508-CFTR[14]. The inhibition of the ΔF508-CFTR-2RK thermal inactivation by VX-809 or C18 suggests that these correctors can directly interact with the mutant at the single molecule level. Although VX-809 prevented the functional inactivation upon raising the temperature from 24°C to 36°C, extended exposure to 36°C attenuated the VX-809- rescue effect probably due to the stabilization of only the NBD1-MSD1/2 interface defect. This interpretation is consistent with the modest effect of NBD1-MSD1/2 interface genetic stabilization[49], compared to that of the NBD1[35], and may explain the negligible effect of VX-809 on the ΔF508-CFTR-I539T thermal inactivation reported recently[38]. Notably, direct interaction of C3 as well as potentiators P1 and VX-770 with purified CFTR was also inferred based on their modulation of the channel ATPase and transport activity[24,50,51].

Definitive identification of VX-809 binding site(s) in the absence of a functionally inert, cross-linkable adduct remains a challenge and is further exacerbated by the coupled folding and misfolding mechanism of CFTR domains[6,8] that may allow allosteric corrections of folding defects from different binding sites. However, our analysis by *in silico* predictions, in concert with *in vitro* assays (DSF and HDX-MS) using isolated human NBD1s and *in vivo* studies using full-length CFTRs with deletion and point mutations, suggest that the NBD1-CL1/4 represents a primary target of VX-809, a conclusion that partly overlaps with a recent proposition[38].

Importantly, mutations confined to the TM helix-1 (G91R) and CL2 (M266R, W277R) of MSD1 could also be partially rescued, presumably via targeting the coupled interface defect at the NBD1-CL1/4. These results, jointly with those obtained using CFTR fragments and CL1 mutations, provide a plausible model of VX-809 action that binds to MSD1 and stabilizes the CL1-CL4 coupling helix, a critical step to form the proper interactions of NBD1 first with MSD1 then with MSD2 and ultimately facilitate cooperative domain assembly upon completion of NBD2 translation[27,28,38]. Counteracting the processing defect of the CF causing R170G and other missense mutation localized to the TM helix-1 and CL1/4 described here and previously[38] by class-I correctors also suggests that VX-809 may be successfully utilized alone or in combination in a variety of rare CF mutations.

While the additive effect of corrector pairing has been previously observed[14,47,48], the rationale for corrector combination remained elusive. Our most important finding is that mechanism-based classification of correctors permitted a rationally designed corrector combination approach that achieved a significant improvement in ΔF508-CFTR rescue efficiency. Chemical correction of NBD1, NBD1-MSD1/2 interface, and NBD2 instabilities almost completely restored the ΔF508-CFTR folding, PM expression, stability, and function in BHK cells. The ΔF508-CFTR rescue was weaker in kidney and respiratory epithelial cells (10–30% of the WT) than in BHK cells. This could be attributed to modest NBD1 stabilization by reduced glycerol concentration (5%) that was required to maintain epithelial polarity.

While the robust combination correction of ΔF508-CFTR transport function in human *CFTR*$^{\Delta F508/\Delta F508}$ organoids may be an overestimate due to the rate limiting ion transport capacity of the basolateral PM in WT intestinal organoid, the VX-809-induced ΔF508-CFTR chloride transport was augmented almost 4-fold by class-II compound and CC based on the FIS measurements. Considering that VX-809 improves ΔF508-CFTR PM function to ~15% of WT in primary human bronchial epithelia[14] with marginally translatable clinical benefit[21], it is reasonable to assume that structural defect-targeted corrector combination will eventually confer sufficient CFTR transport capacity in respiratory epithelial cells to achieve significant clinical improvements in most *CFTR*$^{\Delta F508/\Delta F508}$ patients.

None of the available correctors but CCs can counteract the human ΔF508-NBD1 conformational defect according to *in vitro* and *in vivo* folding studies. This represents a bottleneck of CF pharmacological therapy, since systemic administration of CCs is not feasible. To achieve improved pharmacological corrections in combination with class-I correctors (e.g. VX-809), identification of NBD1 stabilizer is required. Initial isolation of PCs stabilizing the NBD1 could be envisioned by high-throughput screening (HTS) of diverse compounds or fragment libraries *in vitro*, *in vivo* or *in silico* using ΔF508-NBD1 or ΔF508-CFTR cell-based functional or biochemical assays[17,22]. Exploiting NBD1-MSD1/2 interface stabilization by second site suppressor mutation or class-I correctors (e.g.VX-809) may bias HTS efforts towards the isolation of NBD1 stabilizing small molecules. We believe that the successful identification of NBD1 stabilizer would make the mechanism-based corrector combination therapy feasible for most CF patients.

Online Methods

Cell lines

Full-length and truncated human CFTR variants with the 3HA-tag in the 4th extracellular loop[52] were constructed by PCR mutagenesis (Supplementary Table 2). Detailed information on PCR mutagenesis is available from the authors on request. BHK cells stably expressing CFTR variants were generated and grown as previously[27]. MDCK type II cells stably expressing CFTR-3HA variants were generated by lentivirus infection under

puromycin selection (1–5 μg/ml) and grown in Dulbecco's modified Eagle's medium (DMEM) (Invitrogen, Carlsbad, CA) supplemented with 10% fetal bovine serum (FBS). CFBE41o- Tet-on and NCI-H441 Tet-on cells stably expressing CFTR-3HA variants under tetracycline responsive promoter were generated by lentivirus transduction using the Lenti-X TetON Advanced Inducible Expression System (Clontech, Mountain View, CA) under puromycin (3 μg/ml) and G418 selection (0.2 mg/ml) and grown in minimal essential medium (MEM, Invitrogen) supplemented with 10% FBS, 2 mM L-glutamine and 10 mM HEPES, and RPMI-1640 Medium (ATCC) supplemented with 10% FBS. For propagation, the CFBE41o- cells were cultured in plastic flasks coated with an extracellular matrix (ECM mix) consisting of 10 μg/ml human fibronectin (EMD), 30 μg/ml PureCol collagen preparation (Advanced Biomatrix) and 100 μg/ml bovine serum albumin (Sigma-Aldrich) diluted in LHC basal medium (Invitrogen). The CFTR-3HA expression was induced by 0.5 or 1 μg/ml doxycycline treatment for 4 days.

Antibodies and Reagents

Antibodies (Abs) were obtained from the following sources. Monoclonal anti-CFTR Ab L12B4 (recognizing NBD1) and M3A7 (recognizing NBD2) were purchased from Millipore Bioscience Research Reagents (Temecula, CA). Mouse monoclonal anti-HA Ab was from Covance Innovative Antibodies (Berkeley, CA). Chemicals were obtained from Sigma-Aldrich (St. Louis, MO) at the highest grade available. Most of the CFTR correctors were obtained from Cystic Fibrosis Foundation Therapeutics (CFFT), VX-809 from Selleck (Houston, TX), class II compounds were synthesized as described[42]. All of the correctors used in this study are listed in Table S1.

NBD1 protein purification

Recombinant human NBD1 proteins were purified from *E. coli* as previously described[27]. The NBD1 protein was concentrated to 3–5 mg/ml in buffer containing 150 mM NaCl, 1 mM ATP, 2 mM $MgCl_2$, 1 mM TCEP, 10% Glycerol and 10 mM HEPES, pH 7.8.

Microsome Preparation

Microsomes were isolated by differential centrifugation from BHK cells stably expressing 3HA-tagged WT or ΔF508-2RK CFTR as described[27]. To enrich for the complex-glycosylated ΔF508-2RK CFTR, cells were incubated at 26°C for ~36 hours followed by treatment with 150 μg/ml cycloheximide (CHX, 26°C for 12 h) before microsome isolation[52]. WT CFTR expressing cells were treated with 150 μg/ml CHX for 3 hours to eliminate the ER-localized core-glycosylated form.

Planar lipid bilayer studies

WT or ΔF508 CFTR reconstitution and channel activity were essentially measured as described previously[27]. A planar phospholipid bilayer was made of a 2:1 (w/w) mixture of 1-palmitoyl-2-oleoyl-sn-glycero-3-phosphoethanolamine (POPE) and 1-palmitoyl-2-oleoyl-sn-glycero-3-phospho-L-serine (POPS, Avanti Polar Lipids, Alabaster, AL) in n-decane solution at a final lipid concentration of 25 mg/ml and formed over a 200 or 250 μm diameter hole in a polystyrene chamber by monitoring the increase in its capacitance to 150–200 pF. The bilayer was bathed in symmetrical 300 mM Tris-HCl, 10 mM HEPES (pH 7.2), 5 mM $MgC1_2$, and 1 mM EGTA. Microsomes (10–20 μg proteins) isolated from CFTR expressing BHK cells were prephosphorylated in the presence of 100U/ml protein kinase A (PKA) catalytic subunit (Promega) and 2 mM MgATP at room temperature for 10 min, added to the cis compartment and fused to planar lipid bilayer. CFTR channel activity was recorded in the presence of 100 U/ml PKA catalytic subunit and 2 mM MgATP. Currents were measured with a BC-535 amplifier (Warner Instrument, Hamden, CT). Voltage was

clamped at V_m = −60 mV. In temperature ramp experiments the chamber was heated from room temperature to 36°C at a rate of ~1–2°C/min. Single channel activities were acquired using pClamp 8.1 (Axon Instruments) with 10 kHz, filtered at 200 Hz with low pass 8 pole Bessel filter and stored digitally. Records were filtered at 50 Hz and analyzed using Clampfit 10.3 (Axon Instruments). We applied 50% cut off between open and closed levels and events shorter than 10 ms were excluded from the analysis. Single channel open probability (P_o) was determined as NP_o divided by the number of channels, where NP_o was obtained from event detection features of Clampfit 10.3 and N represents the number of channels.

HDX-MS

Localized conformational dynamics of isolated NBD1s was measured by HDX-MS essentially as described[44]. HDX was initiated by mixing 1–2 μL of NBD1 stock solution to 15 volumes of D_2O-based buffer (pD 7.5, based on pD = pH_{read} + 0.40)[53] containing 150 mM NaCl, 1 mM ATP, 2 mM $MgCl_2$, 1 mM TCEP and glycerol, resulting in a final D_2O concentration of more than 90 % (v/v). The final concentration of glycerol was adjusted to 1%. The mixtures were incubated for 15 sec, 1min, 5 min, 15 min, 1 h and 2 h at room temperature and then quenched by adding a 2–2.5 μL aliquot of the mixture to 300 mM phosphate buffer containing 8 M urea, pH 2.5 (quenching buffer). Quenched solutions were flash frozen in MeOH containing dry ice and samples were stored at -80°C.

Prior to high performance liquid chromatography (HPLC)-MS analysis, the labeled protein solutions were thawed, and immediately loaded onto the injection valve. Deuterated NBD1 was digested in an on-line immobilized pepsin column prepared in-house. On-line pepsin digestion was carried out at flow rate of 50 μL/min for ~1.5 min, and resulting peptides were trapped on C18 trapping column (Optimized Technologies, Oregon city, OR). Following desalting for 1.5 min (at 150 μl/min flow rate), peptides were loaded onto a C18 column (1 mm i.d. × 50 mm, Thermo Fisher Scientific, Waltham, MA) through a six-port valve. Peptides were separated using a 13–90% linear gradient of acetonitrile containing 0.1% formic acid for 6 min at 50 μl/min. Chromatographic separation was performed using an Agilent 1100 HPLC system. To minimized back-exchange, the column, solvent delivery lines, injector and other accessories were immersed in an ice bath. The C18 column was directly connected to the electrospray ionization source of LTQ Orbitrap XL (Thermo Fisher Scientific). Mass spectra of peptides were acquired in positive-ion mode for m/z 200–2000. Identification of peptides was carried out in separate experiments by tandem MS (MS/MS) analysis in data-dependent acquisition mode and using collision-induced dissociation. All MS/MS spectra were analyzed using SEQUEST program (Thermo Fisher Scientific). Searching results from SEQUEST were further manually inspected and only those verifiable were considered in HDX analysis. Triplicate measurements were carried out for each time point. HDExaminer (Sierra Analytics, Modesto, CA) were used to determine the deuteration level as a function of labeling time. The deuterium level of peptides were not corrected for back-exchange, and therefore presented values reflect the relative exchange levels across the protein samples[54].

Differential scanning fluorimetry (DSF)

Melting temperature of recombinant human NBD1 was measured as previously[27]. DSF scans of NBD1 (7–12 μM) were obtained in 150 mM NaCl, 20 mM $MgCl_2$, and 10 mM HEPES, pH 7.5 and were performed using a Stratagene Mx3005p (Agilent Technologies, La Jolla, CA) qPCR instrument in the presence of 2X Sypro Orange. The medium ATP concentration was kept at 2.5 mM unless otherwise indicated.

Measurement of CFTR cell surface density and stability

Cell surface CFTR-3HA density and stability was measured by ELISA using anti-HA Ab as previously[52]. The PM density of CD4-NBD1 chimeras was measured by cell surface ELISA using anti-CD4 (OKT4) Ab in transiently transfected COS-7 cells as described[6,27]. Cell surface density of CFTR and CD4-NBD1 chimeras was normalized with protein concentration based on BCA assay. Data were presented as mean values ± SEM from at least 2 independent experiments that consist of multiple (3–8) measurements.

Western blotting and pulse-chase experiments

Western blotting and pulse-chase experiments were performed as previously[52]. Cells were treated with correctors for 24 h at 37°C and during the pulse-labeling and chase period.

Apical Cl^- current (ICl(apical)) measurement

Apical Cl^- current measurements was essentially performed as described[13]. CFBE41o- cells were plated on ECM-mix coated 12 mm Snapwell filters (Corning, Corning, NY) at a density of 1×10^5 cells/cm^2. Polarized epithelia (≥ 5 days post confluence) were mounted in Ussing chambers, bathed in Krebs-bicarbonate Ringer and continuously bubbled with 95% O_2 and 5% CO_2. To impose a chloride gradient, Cl- was replaced by gluconate in the apical compartment. To functionally isolate the apical PM, the basolateral PM was permeabilized with 100 μM amphotericin B and the epithelial sodium channel was inhibited with 100 μM amiloride. CFTR activity was stimulated by apical forskolin (0.03–10 μM) and genistein (100 μM) followed by the addition of CFTR inhibitor 172 (Inh_{172}, 20 μM) to determine CFTR-specific apical Cl^- current (ICl(apical)). Measurements were performed at 37°C. The transepithelial resistance (TER) of CFBE was predominantly between 200–1700 Ω/cm^2. Although combination of three chemicals, including glycerol, reduced the TER of permeabilized CFBE cells to <200 Ω/cm^2, the CFTR-mediated ICl(apical) was measured by monitoring only the CFTR-Inh_{172}-sensitive component of the forskolin and genistein stimulated ICl(apical).

In silico docking

In silico docking of VX-809, C4 and core-corr-II was performed using *AutoDock* 4.2.

Preparation of the proteins—Proteins were prepared initially in PDB format. The structure of the ΔF508-NBD1 was obtained from the PDB database (PDBID:2BBT)[44]. The F504N and Q646R solubilizing mutations were reverted back to F504 and Q646 followed by energy minimization in *SYBYL* (Tripos Inc.) using the AMBER force-field[55] with AMBERF99 charges[56]. Two full-length models, one representing the closed state (http://dokhlab.unc.edu/research/CFTR/home.html)[3], the other representing the open state[36] were selected for docking. For comparability, both models were trimmed to contain amino acids 81–365, 391–648, 855–1154, and 1208–1429. The F508 was deleted followed by the adjustment of the neighboring residues using the *Modloop server*[57] and by energy minimization using the AMBER force-field with AMBERF99 charges[56]. All the amino acid numbers mentioned in the paper correspond to the amino acid numbering in the WT CFTR.

Preparation of ligands—Ligands were prepared in mol2 format. VX-809 was downloaded from the *PubChem Compound Database* in 3D sdf format and converted to mol2 format by *SYBYL*. Molecules C4 and core-corr-II were drawn in 2D using *ChemBioDraw Ultra 12.0* (CambridgeSoft) and saved in mol2 format. Their coordinates were copied to the *PRODRG server*[58] to obtain an initial 3D structure. The resulting mol2 files of C4 and core-corr-II were corrected to contain appropriate atom types and were

subjected to energy minimization in *SYBYL*. Tripos force-field with Gasteiger-Hückel charges were used until the RMS gradient of the energy derivative reached 0.01 kcal/mol/Å.

Running the docking simulations—The docking was performed using *AutoDock*[59]. Input files were prepared using *AutoDock 4.2* with *AutoDockTools* (MGLTools 1.5.4). Ligands were loaded with Gasteiger charges and were saved in pdbqt format. Polar hydrogen atoms and Kollmann charges were added to the proteins. The grid box was centered on coordinates 95 Å, 70 Å, 170 Å and its size was set to 70Å × 70Å × 70Å with 0.5 Å spacing to include the two NBDs and the coupling helices (Fig.S5b). To achieve this box size, AutoDock was compiled with a value of MAX_GRID_POINTS higher than the default 126 that allowed us to set 140 grid points in each direction. Lamarckian Genetic Algorithm was used for docking with default settings, except for the parameters ga_pop_size (300) and ga_num_evals (30,000,000) to perform exhaustive sampling. Three docking simulations with different random seeds for each drug and structure were run on the Hungarian HPC infrastructure (NIIF Institute, Hungary). 250 hits from each run were collected.

Analysis of the docking simulations—All the 750 poses for each docking were used for analysis. These conformations were analyzed using *SciPy* (http://www.scipy.org) and in house written python scripts. A python package for *SciPy* called *hcluster* was used to perform hierarchic clustering based on root means square deviation (RMSD) using the centroid distance measure. The threshold for forming flat clusters was set to include conformations with RMSD values smaller than 3 Å into each cluster. Binding poses were clustered by RMSD and ordered by the binding pose with the lowest binding free energy in each cluster. The four clusters, in which the pose with the lowest binding free energy exhibits one of the lowest binding free energies, are shown in figures, which were prepared in PyMOL (DeLano Scientific LLC). The CFTR amino acid binding sites of correctors were determined using PyMOL by selecting residues in less than 4 Å distance from every molecule in each cluster.

In vitro ubiquitination of NBD1

In vitro ubiquitination of purified ΔF508-1S-NBD1 was performed as previously[27]. NBD1-1S (1 μM) was incubated for 5 min at 34°C with 0.1% DMSO (as control) or C11 in reaction buffer (20 mM HEPES, pH 7.5, 50 mM NaCl, 5 mM $MgCl_2$, 2 mM DTT, 20 μM MG-132, 5 μg/ml leupeptine, 5 μg/ml pepstatin A) in the presence of 2 μM Hsc70. After the heat denaturation, the CHIP-mediated NBD1 ubiquitination was initiated by incubation at 26°C for 2 hours with 0.1 μM E1, 4 μM UbcH5c, 3 μM CHIP and 10 μM ubiquitin (Sigma). NBD1was analyzed by immunoblotting with anti-NBD1 (L12B4) antibody.

Crypt isolation and organoid culture from human rectal biopsies

Crypt isolation and culture of human intestinal organoids have been described previously[60]. Rectal suction biopsies were obtained for intestinal current measurements (ICM) during standard CF care by a procedure described previously[45] that has been approved by the Ethics Committee of the University Medical Centre Utrecht and the Erasmus Medical Centre of Rotterdam. In short, rectal biopsies were washed with cold complete chelation solution and incubated with 10 mM EDTA for 60–120 minutes at 4°C. Supernatant was harvested and EDTA was washed away. Crypts were isolated by centrifugation and embedded in matrigel (growth factor reduced, phenol-free, BD bioscience) and seeded (50–100 crypts per 50 μl matrigel per well) in 24-well plates. The matrigel was polymerized for 10 minutes at 37°C and immersed in complete culture medium: advanced DMEM/F12 supplemented with penicillin/streptomycin, 10 mM HEPES, Glutamax, N2, B27 (all from Invitrogen), 1 mM *N*-acetylcysteine (Sigma) and growth factors: 50 ng/ml mEGF, 50% Wnt3a-conditioned medium and 10% Noggin-conditioned medium, 20% Rspo1-conditioned

medium, 10 μM Nicotinamide (Sigma), 10 nM Gastrin (Sigma), 500 nM A83-01 (Tocris) and 10 μM SB202190 (Sigma). The medium was refreshed every 2–3 days and organoids were passaged 1:4 every 7–10 days. Organoids from passage 1–10 were used for confocal live cell imaging.

CFTR transport activity of human rectal organoids

Organoids were seeded from a 7 day-old culture in 4 μl matrigel placed into a flat-bottom 96-well culture plate (Nunc) and commonly contained 40–80 organoids and 100 μl culture medium. To visualize volume changes, one day after seeding, organoids were loaded with 10 μM calcein-green for 60 min (Invitrogen). After calcein-green treatment (with or without CFTR inhibition), 5 μM forskolin was added and the organoids morphology was monitored by time-lapse fluorescence laser confocal microscopy (LSM710, Zeiss, 5x objective). To inhibit CFTR, organoids were pre-incubated with 50 μM CFTR Inh-172 and 50 μM GlyH-101 (Cystic Fibrosis Foundation Therapeutics, Inc) for 3 h. Images were collected every 10 min for 90 min in a top stage incubator (5% CO_2 at 37°C). Each condition was monitored in triplicate wells. For ΔF508-CFTR correction, organoids were pre-incubated for 20–24 hours with 2 μM C4, 2 μM C18, 100 nM or 2 μM VX-809 or 125 mM myo-inositol (Sigma-Aldrich) as single treatment or in combinations. DMSO concentration was identical under all conditions and did not exceed 0.2 % (w/v). The organoid surface area was quantified using Volocity (Improvision) imaging software. The normalized total organoid surface area was calculated and averaged from three individual wells per condition. The area under the curve (AUC) was calculated using Prism (GraphPad Software).

Statistical analysis

Results are presented as mean ± SEM for the indicated number of experiments. Statistical analysis was performed by two-tailed Student's t-test with the means of at least three independent experiments and the 95% confidence level was considered significant.

Supplementary Material

Refer to Web version on PubMed Central for supplementary material.

Acknowledgments

We thank L. Konerman (Univ. Western Ontario, London, Canada), T. Wales and J. Engen (Notheastern Univ., Boston, USA), M.J. Chalmers and P.R. Griffin (The Scripps Research Institute-Scripps Florida, USA) for valuable advices to set up the HDX-MS technique, D. Gruenert (UCSF, San Francisco, USA) for the parental CFBE41o- cell line, R.J. Bridges (Rosalind Franklin University of Medicine and Science, North Chicago, USA) and the CFFT Inc. for CFTR modulator panels, D. Thomas (McGill University, Canada) for kindly providing RDR compounds and W.R. Skach (Oregon Health and Science University) for advice. We are grateful for the financial support of the Dutch Cystic Fibrosis foundation and the Wilhelmina Children's Hospital Research fund to J.B., the Hungarian National Science Foundation (MB08C-80039 and ERA-Chemistry OTKA grant 102166) to A.S., the EU (FP7-IRG 239270) to T.H., The Tara K. Telford Fund for Cystic Fibrosis Research at the University of California/Davis and The National Institutes of Health (Grants DK072517 and GM089153) to M.K., NIH-NIDDK R01DK75302, CFFT Inc., Cystic Fibrosis Canada, CIHR and CFI to G.L.L. T.H. is a Bolyai Fellow of the Hungarian Academy of Sciences. G.V. was partly supported by an EMBO and FRSQ Fellowship. G.L.L. is a Canada Research Chair.

References

1. Riordan JR. CFTR function and prospects for therapy. Annu Rev Biochem. 2008; 77:701–726. [PubMed: 18304008]
2. He L, et al. Multiple membrane-cytoplasmic domain contacts in the cystic fibrosis transmembrane conductance regulator (CFTR) mediate regulation of channel gating. J Biol Chem. 2008; 283:26383–26390. [PubMed: 18658148]

3. Serohijos AW, et al. Phenylalanine-508 mediates a cytoplasmic-membrane domain contact in the CFTR 3D structure crucial to assembly and channel function. Proc Natl Acad Sci U S A. 2008; 105:3256–3261. [PubMed: 18305154]
4. Kim SJ, Skach WR. Mechanisms of CFTR Folding at the Endoplasmic Reticulum. Front Pharmacol. 2012; 3:201. [PubMed: 23248597]
5. Du K, Sharma M, Lukacs GL. The DeltaF508 cystic fibrosis mutation impairs domain-domain interactions and arrests post-translational folding of CFTR. Nat Struct Mol Biol. 2005; 12:17–25. [PubMed: 15619635]
6. Du K, Lukacs GL. Cooperative assembly and misfolding of CFTR domains in vivo. Mol Biol Cell. 2009; 20:1903–1915. [PubMed: 19176754]
7. He L, et al. Restoration of domain folding and interdomain assembly by second-site suppressors of the DeltaF508 mutation in CFTR. FASEB journal. 2010; 24:3103–3112. [PubMed: 20233947]
8. Cui L, et al. Domain interdependence in the biosynthetic assembly of CFTR. J Mol Biol. 2007; 365:981–994. [PubMed: 17113596]
9. Kleizen B, van Vlijmen T, de Jonge HR, Braakman I. Folding of CFTR is predominantly cotranslational. Mol Cell. 2005; 20:277–287. [PubMed: 16246729]
10. Rosser MF, Grove DE, Chen L, Cyr DM. Assembly and misassembly of cystic fibrosis transmembrane conductance regulator: folding defects caused by deletion of F508 occur before and after the calnexin-dependent association of membrane spanning domain (MSD) 1 and MSD2. Mol Biol Cell. 2008; 19:4570–4579. [PubMed: 18716059]
11. Balch WE, Roth DM, Hutt DM. Emergent properties of proteostasis in managing cystic fibrosis. Cold Spring Harbor perspectives in biology. 2011; 3
12. Boucher RC. New concepts of the pathogenesis of cystic fibrosis lung disease. Eur Respir J. 2004; 23:146–158. [PubMed: 14738247]
13. Veit G, et al. Proinflammatory cytokine secretion is suppressed by TMEM16A or CFTR channel activity in human cystic fibrosis bronchial epithelia. Mol Biol Cell. 2012; 23:4188–4202. [PubMed: 22973054]
14. Van Goor F, et al. Correction of the F508del-CFTR protein processing defect in vitro by the investigational drug VX-809. Proc Natl Acad Sci U S A. 2011; 108:18843–18848. [PubMed: 21976485]
15. Denning GM, et al. Processing of mutant cystic fibrosis transmembrane conductance regulator is temperature-sensitive. Nature. 1992; 358:761–764. [PubMed: 1380673]
16. Sato S, Ward CL, Krouse ME, Wine JJ, Kopito RR. Glycerol reverses the misfolding phenotype of the most common cystic fibrosis mutation. J Biol Chem. 1996; 271:635–638. [PubMed: 8557666]
17. Pedemonte N, et al. Small-molecule correctors of defective DeltaF508-CFTR cellular processing identified by high-throughput screening. J Clin Invest. 2005; 115:2564–2571. [PubMed: 16127463]
18. Varga K, et al. Enhanced cell-surface stability of rescued DeltaF508 cystic fibrosis transmembrane conductance regulator (CFTR) by pharmacological chaperones. Biochem J. 2008; 410:555–564. [PubMed: 18052931]
19. Hanrahan JW, Sampson HM, Thomas DY. Novel pharmacological strategies to treat cystic fibrosis. Trends Pharmacol Sci. 2013; 34:119–125. [PubMed: 23380248]
20. Van Goor F, et al. Rescue of CF airway epithelial cell function in vitro by a CFTR potentiator, VX-770. Proc Natl Acad Sci U S A. 2009; 106:18825–18830. [PubMed: 19846789]
21. Clancy JP, et al. Results of a phase IIa study of VX-809, an investigational CFTR corrector compound, in subjects with cystic fibrosis homozygous for the F508del-CFTR mutation. Thorax. 2012; 67:12–18. [PubMed: 21825083]
22. Sampson HM, et al. Identification of a NBD1-binding pharmacological chaperone that corrects the trafficking defect of F508del-CFTR. Chem Biol. 2011; 18:231–242. [PubMed: 21338920]
23. Howard M, et al. Mammalian osmolytes and S-nitrosoglutathione promote Delta F508 cystic fibrosis transmembrane conductance regulator (CFTR) protein maturation and function. J Biol Chem. 2003; 278:35159–35167. [PubMed: 12837761]
24. Kim Chiaw P, Wellhauser L, Huan LJ, Ramjeesingh M, Bear CE. A chemical corrector modifies the channel function of F508del-CFTR. Mol Pharmacol. 2010; 78:411–418. [PubMed: 20501743]

25. Protasevich I, et al. Thermal unfolding studies show the disease causing F508del mutation in CFTR thermodynamically destabilizes nucleotide-binding domain 1. Protein Sci. 2010; 19:1917–1931. [PubMed: 20687133]
26. Wang C, et al. Integrated biophysical studies implicate partial unfolding of NBD1 of CFTR in the molecular pathogenesis of F508del cystic fibrosis. Protein Sci. 2010; 19:1932–1947. [PubMed: 20687163]
27. Rabeh WM, et al. Correction of both NBD1 energetics and domain interface is required to restore DeltaF508 CFTR folding and function. Cell. 2012; 148:150–163. [PubMed: 22265408]
28. Mendoza JL, et al. Requirements for efficient correction of DeltaF508 CFTR revealed by analyses of evolved sequences. Cell. 2012; 148:164–174. [PubMed: 22265409]
29. Robert R, et al. Correction of the Delta phe508 cystic fibrosis transmembrane conductance regulator trafficking defect by the bioavailable compound glafenine. Mol Pharmacol. 2010; 77:922–930. [PubMed: 20200141]
30. Loo TW, Bartlett MC, Clarke DM. The V510D suppressor mutation stabilizes DeltaF508-CFTR at the cell surface. Biochemistry. 2010; 49:6352–6357. [PubMed: 20590134]
31. Teem JL, et al. Identification of revertants for the cystic fibrosis delta F508 mutation using STE6-CFTR chimeras in yeast. Cell. 1993; 73:335–346. [PubMed: 7682896]
32. Pedemonte N, et al. Dual activity of aminoarylthiazoles on the trafficking and gating defects of the cystic fibrosis transmembrane conductance regulator chloride channel caused by cystic fibrosis mutations. J Biol Chem. 2011; 286:15215–15226. [PubMed: 21383017]
33. Phuan PW, et al. Cyanoquinolines with independent corrector and potentiator activities restore DeltaPhe508-cystic fibrosis transmembrane conductance regulator chloride channel function in cystic fibrosis. Mol Pharmacol. 2011; 80:683–693. [PubMed: 21730204]
34. Hegedus T, et al. F508del CFTR with two altered RXR motifs escapes from ER quality control but its channel activity is thermally sensitive. Biochim Biophys Acta. 2006; 1758:565–572. [PubMed: 16624253]
35. Aleksandrov AA, et al. Allosteric modulation balances thermodynamic stability and restores function of DeltaF508 CFTR. J Mol Biol. 2012; 419:41–60. [PubMed: 22406676]
36. Dalton J, Kalid O, Schushan M, Ben-Tal N, Villa-Freixa J. New Model of Cystic Fibrosis Transmembrane Conductance Regulator Proposes Active Channel-like Conformation. J Chem Inf Model. 2012
37. Kalid O, et al. Small molecule correctors of F508del-CFTR discovered by structure-based virtual screening. J Comput Aided Mol Des. 2010; 24:971–991. [PubMed: 20976528]
38. He L, et al. Correctors of {Delta}F508 CFTR restore global conformational maturation without thermally stabilizing the mutant protein. Faseb J. 2013; 27:536–545. [PubMed: 23104983]
39. Thibodeau PH, et al. The cystic fibrosis-causing mutation deltaF508 affects multiple steps in cystic fibrosis transmembrane conductance regulator biogenesis. J Biol Chem. 2010; 285:35825–35835. [PubMed: 20667826]
40. Grove DE, Rosser MF, Ren HY, Naren AP, Cyr DM. Mechanisms for rescue of correctable folding defects in CFTRDelta F508. Mol Biol Cell. 2009; 20:4059–4069. [PubMed: 19625452]
41. Zhang F, Kartner N, Lukacs GL. Limited proteolysis as a probe for arrested conformational maturation of delta F508 CFTR. Nat Struct Bio. 1998; 5:180–183. [PubMed: 9501909]
42. Yu GJ, et al. Potent s-cis-locked bithiazole correctors of DeltaF508 cystic fibrosis transmembrane conductance regulator cellular processing for cystic fibrosis therapy. J Med Chem. 2008; 51:6044–6054. [PubMed: 18788728]
43. Aleksandrov AA, et al. Regulatory insertion removal restores maturation, stability and function of DeltaF508 CFTR. J Mol Biol. 2010; 401:194–210. [PubMed: 20561529]
44. Lewis HA, et al. Structure and dynamics of NBD1 from CFTR characterized using crystallography and hydrogen/deuterium exchange mass spectrometry. J Mol Biol. 2010; 396:406–430. [PubMed: 19944699]
45. Dekkers J, et al. A functional CFTR assay using primary cystic fibrosis intestinal organoids. Nat Med. in press.

46. Zhang XM, et al. Organic solutes rescue the functional defect in delta F508 cystic fibrosis transmembrane conductance regulator. J Biol Chem. 2003; 278:51232–51242. [PubMed: 14532265]
47. Wang Y, Loo TW, Bartlett MC, Clarke DM. Additive effect of multiple pharmacological chaperones on maturation of CFTR processing mutants. Biochem J. 2007; 406:257–263. [PubMed: 17535157]
48. Pedemonte N, Tomati V, Sondo E, Galietta LJ. Influence of cell background on pharmacological rescue of mutant CFTR. Am J Physiol Cell Physiol. 2010; 298:C866–874. [PubMed: 20053923]
49. Liu X, O'Donnell N, Landstrom A, Skach WR, Dawson DC. Thermal instability of DeltaF508 cystic fibrosis transmembrane conductance regulator (CFTR) channel function: protection by single suppressor mutations and inhibiting channel activity. Biochemistry. 2012; 51:5113–5124. [PubMed: 22680785]
50. Wellhauser L, et al. A small-molecule modulator interacts directly with deltaPhe508-CFTR to modify its ATPase activity and conformational stability. Mol Pharmacol. 2009; 75:1430–1438. [PubMed: 19339490]
51. Eckford PD, Li C, Ramjeesingh M, Bear CE. Cystic Fibrosis Transmembrane Conductance Regulator (CFTR) Potentiator VX-770 (Ivacaftor) Opens the Defective Channel Gate of Mutant CFTR in a Phosphorylation-dependent but ATP-independent Manner. J Biol Chem. 2012; 287:36639–36649. [PubMed: 22942289]
52. Okiyoneda T, et al. Peripheral protein quality control removes unfolded CFTR from the plasma membrane. Science. 2010; 329:805–810. [PubMed: 20595578]
53. Glasoe PK, Long FA. Use of glass electrodes to measure acidities in deuterium oxide. J Phys Chem. 1960; 64:188–189.
54. Wales TE, Engen JR. Hydrogen exchange mass spectrometry for the analysis of protein dynamics. Mass Spectrom Rev. 2006; 25:158–170. [PubMed: 16208684]
55. Cornell WD, Cieplak P, Bayly CI, Gould IR, Merz KM Jr, Ferguson DM, Spellmeyer DC, Xov T, Caldwell JW, Kollman PA. A second generation force field for the simulation of proteins Nucleic Acids and Organic Molecules. J Am Chem Soc. 1995; 117:5159.
56. Wang J, Cieplak P, Kollmann PA. How well does a restrained electrostatic potential (RESP) model perform in calculating conformational energies of organic and biological molecules? J Comput Chem. 2000; 21:1049–1074.
57. Fiser A, Sali A. ModLoop: automated modeling of loops in protein structures. Bioinformatics. 2003; 19:2500–2501. [PubMed: 14668246]
58. Schuttelkopf AW, van Aalten DM. PRODRG: a tool for high-throughput crystallography of protein-ligand complexes. Acta Crystallogr D Biol Crystallogr. 2004; 60:1355–1363. [PubMed: 15272157]
59. Morris GM, et al. AutoDock4 and AutoDockTools4: Automated docking with selective receptor flexibility. J Comput Chem. 2009; 30:2785–2791. [PubMed: 19399780]
60. Sato T, et al. Long-term expansion of epithelial organoids from human colon, adenoma, adenocarcinoma, and Barrett's epithelium. Gastroenterology. 2011; 141:1762–1772. [PubMed: 21889923]

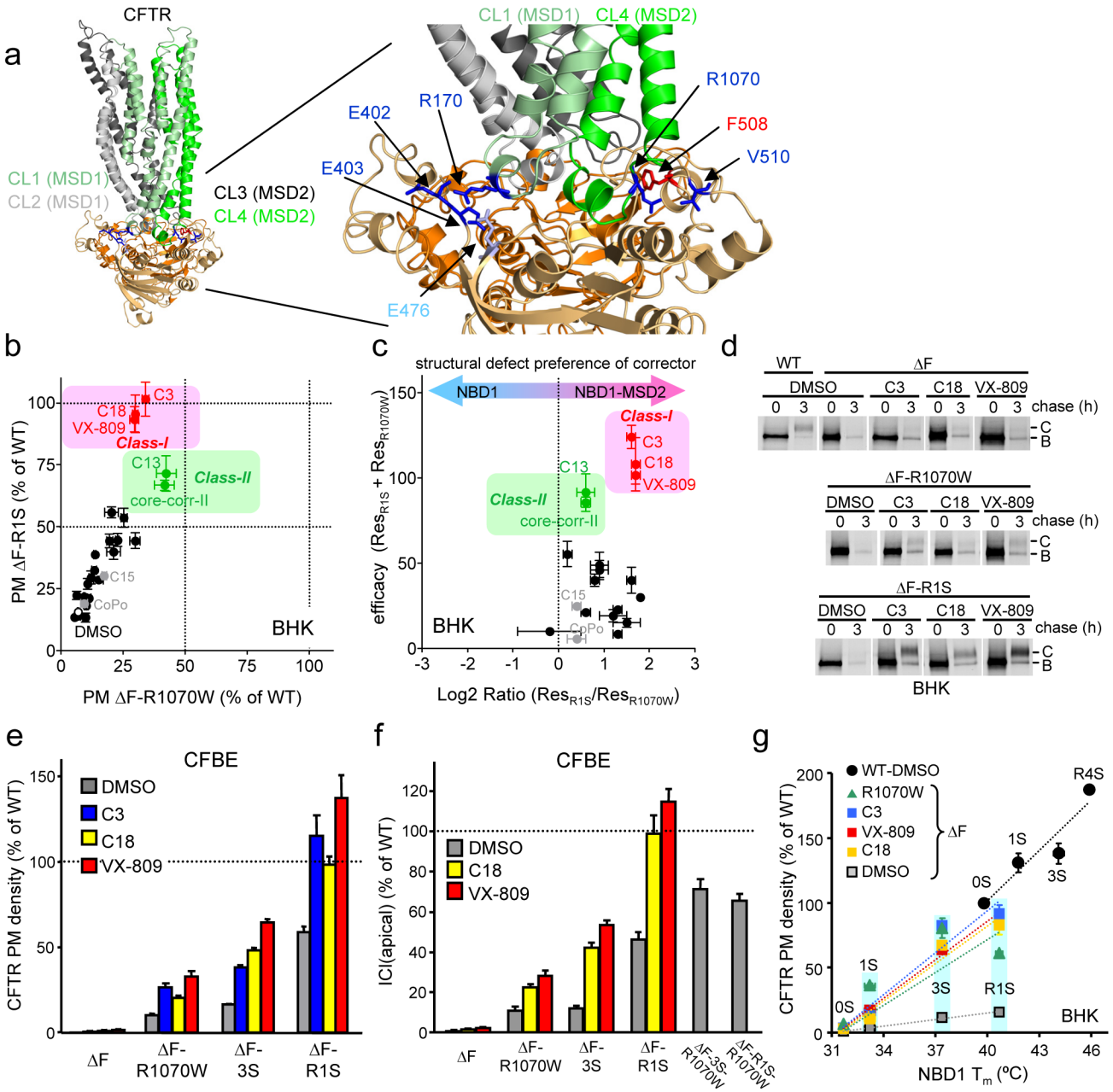

Figure 1. Combination of corrector and suppressor mutations restores ΔF508-CFTR folding, PM expression and function

(a) NBDs-MSDs interfaces in the CFTR open structural model[36]. Some critical interface residues are indicated. (b) Relative PM density of ΔF508-CFTR containing R1S (Y-axis) or R1070W (X-axis) upon corrector treatment was measured by ELISA in BHK cells (n=6–12). Correctors indicated by black symbols are listed in Supplementary Fig. 2a. (c) Structural preference of correctors to NBD1-MSD2 interface over NBD1 stability defect was visualized by plotting sum of correction (Res_{R1S} + Res_{R1070W}, Y-axis) as a function of log_2 ratio of the augmented PM density of ΔF508-CFTR with R1S and R1070W (Res_{R1S}/Res_{R1070W}, X-axis). (d) Maturation efficiency of ΔF508-CFTR was measured by metabolic pulse-chase experiments. B, immature core-glycosylated; C, mature complex-glycosylated

form. (e–f) PM density (e; n=8–20), and function (h; n=3–4) of ΔF508-CFTR with or without suppressor mutation was measured by ELISA and apical Cl^- current (ICl(apical)), respectively, in CFBE41o- cells. Na^+/K^+-ATPase (ATPase) was used as a loading control. (g) Correlation between T_m of NBD1 variants of 0S, 1S, 3S, R1S and R4S (listed in Table S2) and PM density of the respective CFTR variants in BHK cells (n=8–12) in the presence or absence of correctors. The data were fitted by linear regression analysis and slopes were listed in the result as %/°C unit. Correctors (C3 at 10 μM; C18 or VX-809 at 3 μM) were applied for 24 h at 37°C. Data are means ± SEM.

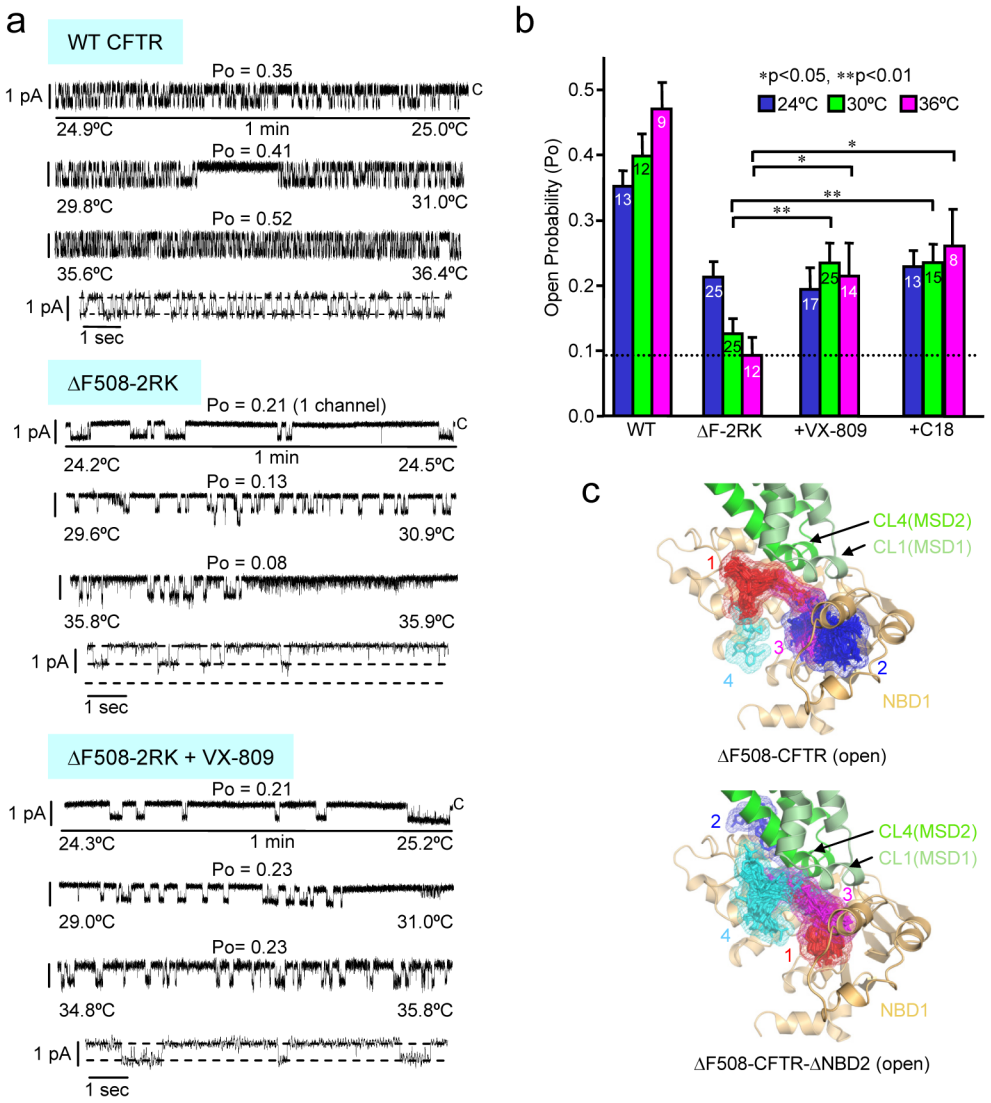

Figure 2. VX-809 functions as a pharmacological chaperone of CFTR

(a-b) Effect of VX-809 and C18 correctors on thermal inactivation of the ΔF508-CFTR-2RK reconstituted into artificial phospholipid bilayer. (a) Representative channel activity is shown for WT or ΔF508-2RK CFTR at 24°C, 30°C or 36°C during the temperature ramp in the absence or presence of 3 μM VX-809. The processing defect of the ΔF508-CFTR variants was rescued at 26°C prior to microsome isolation. Channel activity is also shown at higher time resolution for each condition at 36°C. The closed (c) state of the channels is indicated. The control gating of ΔF508-CFTR-2RK was derived from separate experiments at 24°C and 27°C plus 36°C. Incorporation of two channels was observed at 27–36°C. The ΔF508-CFTR-2RK activity was recorded in separate experiment at 24°C plus 30°C and 36°C in presence of VX-809. (b) The P_o of PKA-activated CFTRs was analyzed at the indicated temperature as described in panel a. Cumulative duration of single channel experiments for WT and ΔF508-CFTR-2RK was at least 15 min. Number of independent experiments is indicated in the bars (n=8–25). Data represent means ± SEM and significance was tested by paired t-test. *<0.05, **p<0.01. (c) VX-809 *in silico* docking to open ΔF508-CFTR (top panel) or ΔF508-CFTR-ΔNBD2 model (bottom panel) obtained by AutoDock. The first four VX-809 clusters are ranked based on their lowest binding energy pose in

ascending order and are illustrated on the model using PyMOL. For clarity, NBD2 and R-domain are hidden from the full-length model. Red, blue, magenta, cyan: clusters of VX-809 with increasing binding free energy.

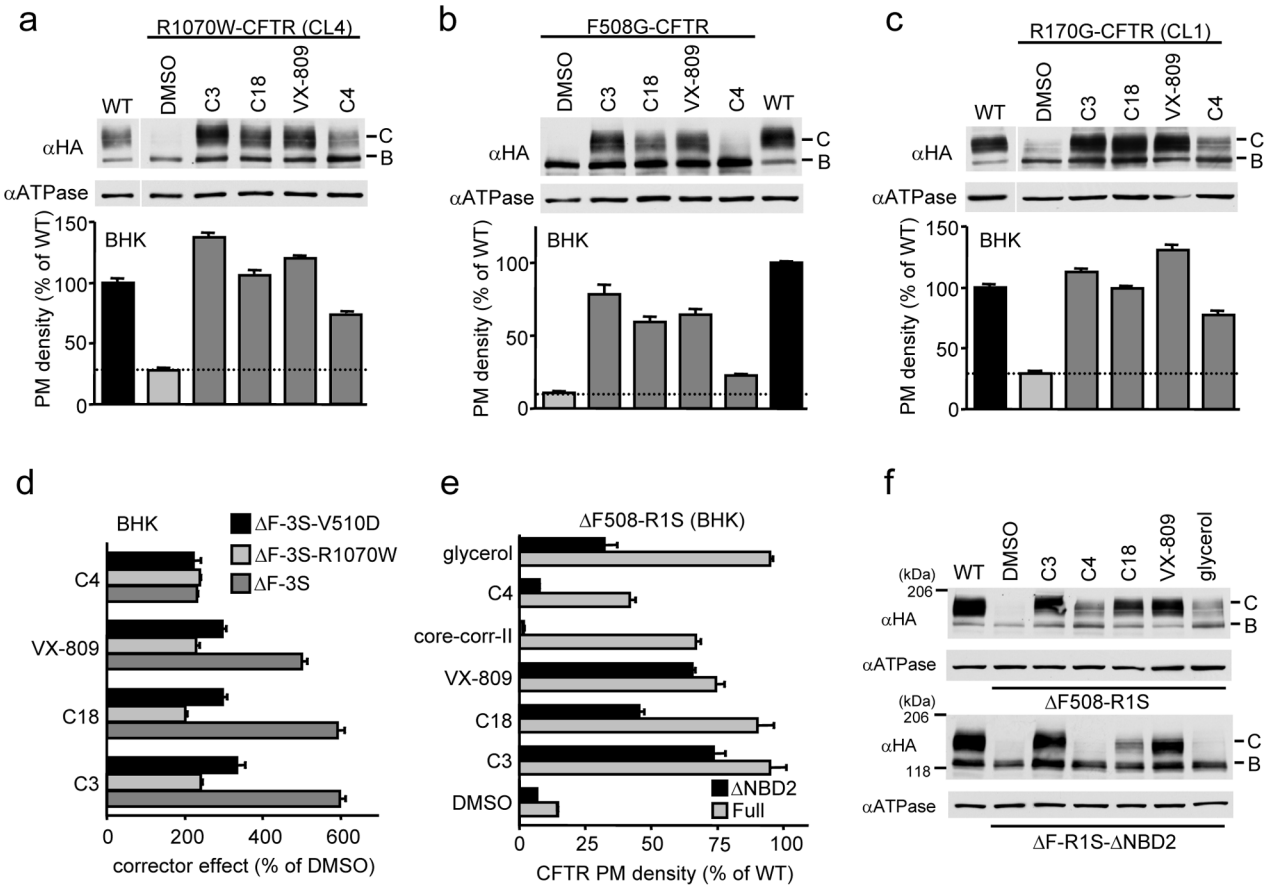

Figure 3. Evaluating corrector mechanism by using CFTR variants

(a–c) Effect of correctors (10 μM C3 or C4, 3 μM C18 or VX-809 for 24 h at 37°C) on cellular expression (upper) and PM density (lower) of R1070W (a), F508G (b), and R170G (c) CFTR variants in BHK cells, measured by Western blotting and cell surface ELISA (n=8), respectively. (d) Effect of V510D or R1070W mutation on the PM density of corrector treated ΔF508-CFTR-3S measured by cell surface ELISA in BHK cells and expressed as % of the respective DMSO control (n=8). Same results are also shown in Supplementary Fig. 6a as % of WT. (e–f) Effect of NBD2 deletion (ΔNBD2) on corrector effect measured by the PM density (e, n=6–9) and cellular expression (f) of ΔF508-CFTR-R1S. Correctors (5 μg/ml core-corr-II, 10% glycerol, others are same as in panel a–c) were added for 24 h at 37°C. Data represent means ± SEM.

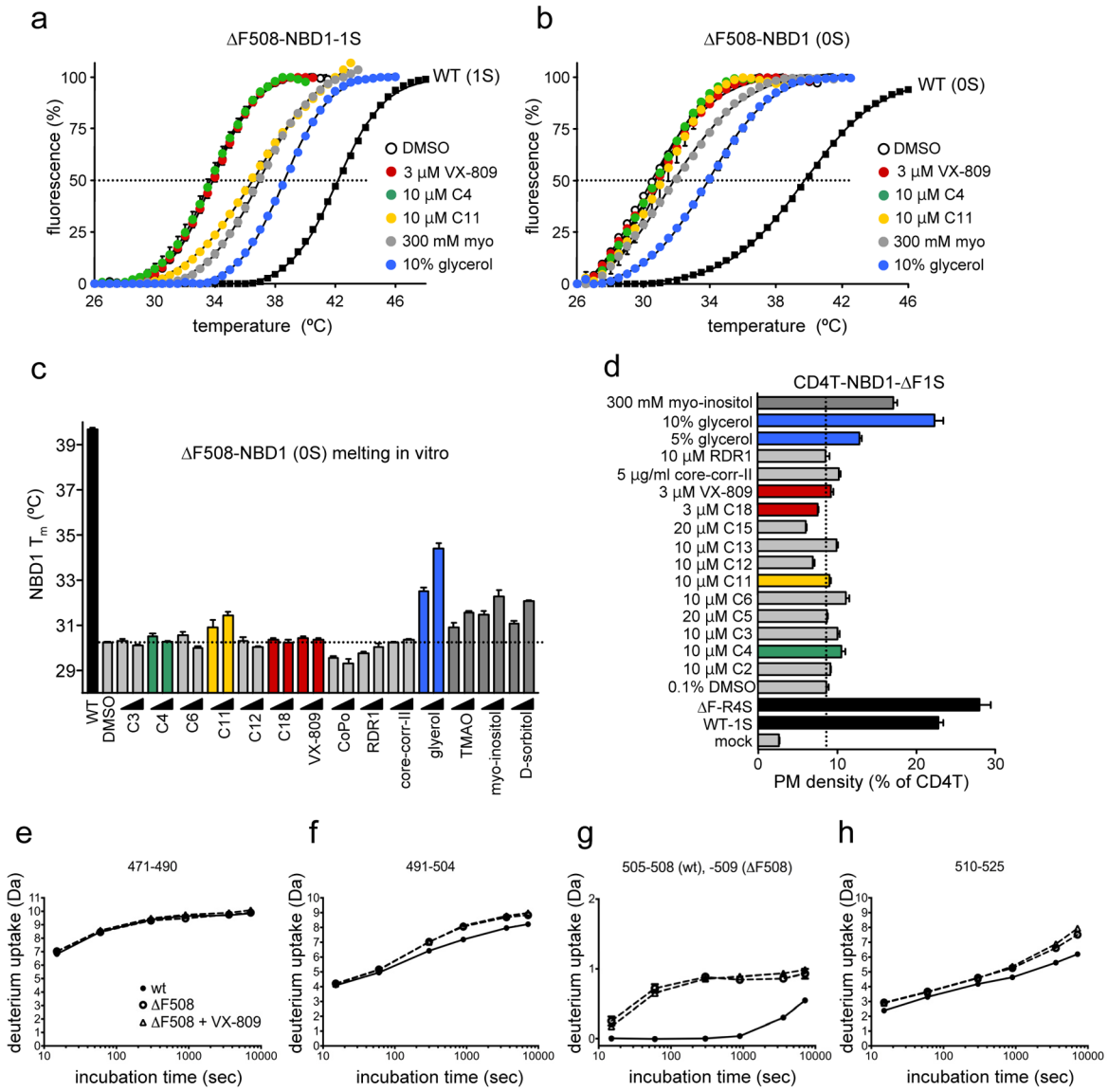

Figure 4. Effect of correctors on the isolated NBD1 stability *in vitro* and *in vivo*

(a–c) Melting temperature (T_m) of human ΔF508-NBD1-1S (a) or ΔF508-NBD1 (b, c) was determined by differential scanning fluorimetry (DSF)[6,27] as described in Methods. The indicated correctors or chemical chaperones (CC) (see Supplementary Table 1) were present during thermal unfolding at the following concentration: 3 μM and 10 μM C1, C2, C3, C4, C5, C6, C7, C9, C11, C12, C13, C14, C17 and CoPo; 10 μM and 20 μM C8, C15 and C16; 1 μM and 3 μM C18 and VX-809, 5 μM and 15 μM RDR1; 2.5 μg/ml and 5 μg/ml core-corr-II; 5% and 10% glycerol; 150 mM and 300 mM TMAO, taurine, myo-inositol and D-sorbitol. WT-NBD1-1S or WT-NBD1 was used as a positive control. (c) T_m of ΔF508-NBD1 was determined by DSF as in panel b. Data represent mean ± SEM (n=3). Change in T_m was considered statistically significant if they were > ± 3SD (30.2 ± 0.4°C) of DMSO treated ΔF508-NBD1 T_m. (d) PM density of CD4T-ΔF508-NBD1-1S in COS7 cells was measured by PM ELISA using anti-CD4 Ab. The ELISA signal of mock-transfected cells is also indicated. Cells were treated with corrector for 24 h at 37°C. CD4T-WT-NBD1-1S (WT-1S) and CD4T-ΔF508-NBD1-R4S (ΔF-R4S) were used as positive control. Data

represents mean ± SEM (n=8–12). (eh). Conformational dynamics of wt and ΔF508-NBD1-1S was determined by HDX-MS following 5 min D_2O labelling in the presence or absence of 10 μM VX-809. Data are means ± SEM (n=3). Representative peptides are shown from > sixty peptides obtained by pepsin digestion.

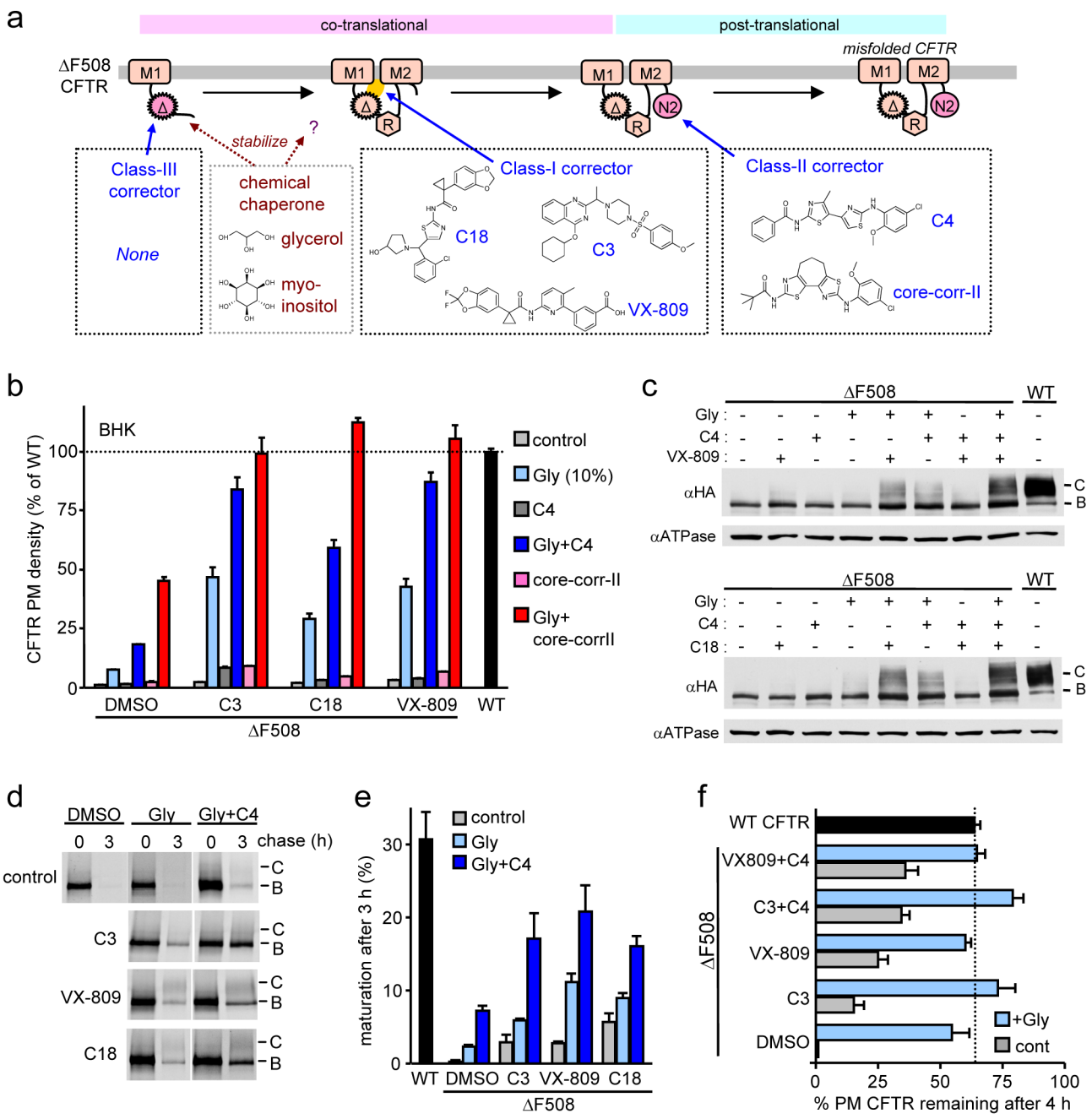

Figure 5. Combination of correctors targeting distinct structural defects completely restores ΔF508-CFTR folding, PM expression and stability in BHK cells

(a) Schematic model shows the proposed targets of available correctors based on *in vitro*, *in vivo* and *in silico* analysis. Chemical chaperones (CC, e.g. glycerol and myo-inositol) preferentially, but presumably not exclusively stabilize the ΔF508-NBD1. VX-809, C18 and C3 target the NBD1-MSD1/2 interface and C4 and core-corr-II target the NBD2. (b–f) ΔF508-CFTR PM density (b; n=6–12), cellular expression (c), ER folding efficiency (d–e; n=3–4) and PM stability after 4 h (f; n=5–12) were determined upon treatment with correctors (10 μM C3 or C4; 3 μM C18 or VX-809, 5 μg/ml core-corr-II; 10% glycerol) or

their combinations in BHK cells by cell surface ELISA, Western blotting, metabolic pulse-chase technique and cell surface ELISA, respectively. All data represent means ± SEM.

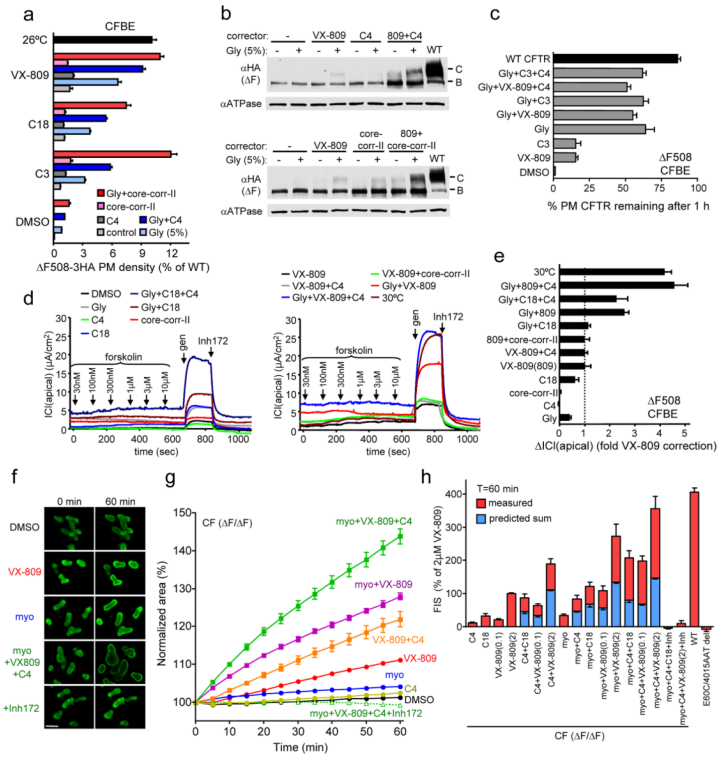

Figure 6. Corrector combination restores ΔF508-CFTR functional expression in polarized epithelial cell lines and rectal organoids from ΔF508 CF patients

(a–e) ΔF508-CFTR PM density (a, n=7–22), cellular expression (b), PM stability (c, n=16) and function (d, n=3–4) in CFBE41o- cells. Correctors (10 μM C3 or C4, 3 μM C18 or VX-809, 2.5 μg/ml core-corr-II, 5% glycerol [Gly]) were applied for 24 h at 37°C. For comparison, ΔF508-CFTR was rescued by low temperature at 26°C or 30°C for 36–48 h. (d) Representative records of forskolin and 100 μM genistein (gen) activated ΔF508-CFTR ICl(apical) following corrector treatment are shown. (e) Summary of the peak, Inh_{172}-sensitive ICl(apical) of ΔF508-CFTR in CFBE41o- cells after corrector treatment (n=3–4). (f) Fluorescence laser confocal images of calcein-green loaded CF rectal organoids before and after forskolin-induced swelling (FIS) for 60 min in the presence of correctors (2 μM, VX-809, C4 and/or 125 mM myo-inositol (myo)), and inhibitor (Inh; 50 μM CFTR inhibitor-172 and GlyH-101). (g) Time course of FIS of CF organoids from a representative experiment. Organoids were treated as described in Methods. FIS was expressed as percentage of initial cell cross-sectional area before forskolin stimulation. (h) FIS was expressed as percentage of the area of 2 μM VX-809 treated cells after 60 min of FIS. Besides the measured FIS (red bar), the predicted sum of the individual corrector effect (2 μM C3, C4, C18; 0.1 or 2 μM VX-809; 125 mM myo-inositol) is indicated, assuming additive effect (blue bar). The mean FIS from three healthy controls (WT) is included. No FIS was observed after treatment of myo-inositol, C4 and VX-809 in organoids carrying E60X/4015ATTdel CFTR mutant. Data represent means ± SEM from six independent experiments performed on three ΔF508 homozygous patients.